

RESEARCH ARTICLE

Gallium Nanoparticle-Mediated Reduction of Brain Specific Serine Protease-4 in an Experimental Metastatic Cancer Model

Enas M Moustafa^{1*}, Marwa Abdelhameed Mohamed², Noura M Thabet¹

Abstract

Purpose: Tumor growth and metastasis depend on angiogenesis; therefore, efforts are being made to develop specific angiogenic inhibitors. Gallium (Ga) is the second most common metal ion, after platinum, used in cancer treatment. Its activities are numerous and various. In the present study, we aimed to investigate the effect of Ga on brain metastasis arising from hepatocellular carcinoma (HCC). **Materials and methods:** Forty experimental rats (divided into 4 groups) received diethylnitrosamine (DEN) at a dose (20 mg/kg.b.wt.; for 6 weeks) to induce HCC and were treated with Ga nanoparticles (GaNPs) with the bacterium *Bacillus licheniformis* (1mg/kg.b.wt.). Liver functions (alanine aminotransferase; (ALT), aspartate aminotransferase; (AST) and gamma glutamyl transferase; (GGT) and alpha-fetoprotein (AFP)) were assessed with histopathological examination of liver sections to confirm the induction of HCC. In addition, brain-specific serine protease 4 (BSSP4), extracellular signal-regulated kinase (ERK), a microtubule-associated protein (Tau), vascular endothelial growth factor (VEGF), vascular cells adhesion molecule-1 (VCAM-1), cytochrome P450 (CYP450), lipid peroxidation (MDA) and glutathione-S-transferase (GST) were measured in brain tissue. **Results:** GaNPs ranged from 5 to 7 nm. HCC was confirmed by elevation in liver enzymes and AFP. Additionally, histopathological examination of liver showed focal area of anaplastic hepatocytes with other cells forming acini associated with fibroblastic cell proliferation. In brain, compared to the DEN alone group, we found that GaNPs modulated brain metastasis by reducing CYP450 and BSSP4 mRNA, and protein expression of p-ERK and p-Tau, and angiogenesis mediators (VEGF and VCAM-1). Also, GaNPs elevated lipid peroxidation and GST activity. **Conclusion:** It is concluded that GaNPs may prevent metastasis via inhibition of BSSP4 mRNA expression leading to suppression of a variety of growth factors and cell adhesion molecules involved in tumor growth and angiogenesis.

Keywords: DEN- GaNPs- AFP- BSSP4- p-ERK- VEGF

Asian Pac J Cancer Prev, **18 (4)**, 895-903

Introduction

Nitrosamines are ubiquitous in the human environment and have been detected in food items, including cured meat, fish, beer, and in drugs (Lijinsky, 1999). Also, exposure to nitrosamines occurs through manufacturing and processing of rubber and latex products, as well as fertilizers, pesticides and cosmetics. Nitrosamines, formed by chemical reactions between nitrites and secondary amines or proteins, exert their toxic and mutagenic effects by alkylating N-7 of guanine and generation of reactive oxygen species (ROS) such as superoxide (O₂⁻) and hydrogen peroxide (H₂O₂), which result in increased lipid peroxidation, protein adduct formation, increased DNA damage and pro-inflammatory cytokine activation (Pegg, 1980; Espey et al., 2002). Diethylnitrosamine (DEN), also known as N-nitrosodiethylamine, is widely used as a carcinogen in experimental animal models (Rajan et al., 2015). Exposure to alkylating agents could result in malignancy and/or tissue degeneration is not

far-fetched. Chronic exposure to tobacco nitrosamines causes both lung cancer and emphysema with chronic obstructive pulmonary disease and exposures to a nitrosamine-related compound like Streptozotocin, can cause hepatocellular or pancreatic carcinoma, Type 2 diabetes, Alzheimer's -type neurodegeneration and Parkinson's or hepatic steatosis (Lester-Coll et al., 2006; Szkudelski, 2001). Hepatocellular carcinoma (HCC) is one of the most common cancers worldwide with highly malignant neoplasms. It is the fifth most common form of cancer globally and the third most common cause of cancer-related deaths. HCC commonly metastasizes to the lung, regional lymph nodes, peritoneum, and adrenal glands, but rarely to brain (Tunc et al. 2004; Park et al., 2014). Also, cases report of Tunc et al., (2004) study concluded that the rarity of brain metastases arising from HCC gives the clinician the suspicion of such associations when confronted with a patient with liver dysfunction and neurologic findings. Additionally, therapeutic advances in the management of HCC have improved the survival

¹Radiation Biology Department, ²Drug Radiation Research Department, National Center for Radiation Research and Technology, Atomic Energy Authority, Cairo, Egypt. *For Correspondence: inas.mahmoud@live.com

of patients with the disease. Therefore, the incidence of brain metastases from HCC is expected to increase (Park et al., 2014).

Brain-specific serine protease 4 (BSSP4) is a member of serine proteases of the trypsin-like family have long been recognized to be critical effectors of biological processes as diverse as digestion, blood coagulation, fibrinolysis and immunity (Antalis et al., 2011). Its mRNA was expressed exclusively in the white matter of the cerebellum, medulla oblongata and capsula interna and capsula interna pars retrolenticularis of brain under normal physiological conditions (Matsui et al., 2000). Yasuda et al., (2005) demonstrated that BSSP4 catalyzes the progression of zymogen pro-uPA to form active (uPA) urokinase-type plasminogen period. Moreover, the uPA-uPAR system has been linked to the mitogen-activated protein kinase/extracellular signal-regulated kinase (ERK) signaling pathway. ERK kinases are a major determinant in the control of diverse cellular processes such as proliferation, survival and motility (Kohno et al., 2011).

Gallium nitrate is a simple metal salt that can be considered to belong to a first generation of gallium compounds (Bonchi et al., 2014). The chemical characteristics of the Ga³⁺ ion and its ability to interfere with several cellular functions rendered this metal very attractive for biomedical scientists, paving the way to a number of therapeutic applications. The therapeutic properties of gallium led to the development of novel formulations for treatment of various disorders in humans, including cancer, autoimmune diseases, accelerated bone resorption and infectious diseases (Chitambar, 2010). Nanoparticles can be defined as particulate dispersions or solid particles with a size in the range of 10-1000 nm (Nagavarma et al., 2012). Nanoparticles will be able to deliver a concentrate dose of drug via the enhanced permeability and retention effect (Mohanraj and Chen, 2006).

In the present study, we aimed to investigate the effect of Ga nanoparticles (GaNPs) on brain metastasis arising from hepatocellular carcinoma (HCC). To induce HCC, we demonstrate diethylnitrosamine (DEN) (for 6 weeks) and then treated with GaNPs. Liver functions (alanine aminotransferase; (ALT), aspartate amino transferase; (AST) and gamma glutamyl transferase; (GGT) and Alpha-fetoprotein (AFP) with histopathological examination of liver sections were confirmed the induction of HCC. Besides, Brain-specific serine protease 4 (BSSP4), extracellular signal-regulated kinase (ERK), The microtubule-associated protein (Tau), vascular endothelial growth factor (VEGF), vascular cells adhesion molecule-1 (VCAM-1), cytochrome P450 (CYP450), lipid peroxidation (MDA) and glutathione-S-transferase (GST) were done in brain tissue to investigate the effect of GaNPs on brain metastasis.

Materials and Methods

Diethylnitrosamine (DEN) was obtained from Sigma-Aldrich Chemical Co., St. Louis, Mo. USA. Also, all chemicals and reagent were obtained from Sigma-Aldrich.

Preparation and Verification of Gallium Nanoparticles

Gallium nanoparticles (GaNPs) produce from isolated bacterium *Bacillus licheniformis*, collected from municipal wastes in sterilized falcon tubes. They were serially diluted and spread on nutrient agar plates. The plates were then incubated at 37 °C for 48 h. The morphological and physiological characterization of the strictly aerobic isolate was performed according to the methods described in Bergey's manual of determinative bacteriology (Holt et al., 1994). The characterized isolate was inoculated into sterile nutrient broth (NB) and 2 g of wet biomass was harvested at different points of time. The biomass obtained was washed with phosphate buffer (pH 7.0) thrice and collected in a 500-ml Erlenmeyer flask. A 1- mM solution of GaNO₃ was prepared using deionized water, and 100 ml of the solution was added to the biomass harvested at each point of time. The Erlenmeyer flasks were incubated at 37 °C under agitation (200 rpm) for 24 h. The cells from each Erlenmeyer flask were washed twice with 50mM phosphate buffer (pH 7.0) and suspended in 1 ml of the same buffer. Ultrasonic disruption of cells was carried out with an ultrasonic processor (Sonics Vibra Cell VC-505/220, Newtown, USA) over three 15 s periods, and with an interval of 45 s between periods. The sonicated samples were centrifuged at 15,000 rpm for 30 min at 4°C to remove cell-debris. The resulting aqueous solution was filtered through a 0.22 µm Millipore filter before use according to Philip, (2009). Verification of GaNPs was carried out by:

1. Fourier Transform Spectroscopic Infrared (FT-IR) technique (JASCO FT-IR 6300).
2. Transmission Electron Microscope (TEM) (JEOL Electron Microscope, JEM-100CX) (Huang et al., 2003).

Acute toxicity studies and determination of median lethal dose (LD50)

Traditionally, acute oral toxicity testing has focused on determining the dose that kills half of the animals (i.e., the median lethal dose or LD50), the timing of lethality following acute chemical exposure, as well as observing the onset, nature, severity, and reversibility of toxicity (Hodgson, 2010). The optimum selected dose for evaluating the in vivo antitumor activity of the novel synthesized GaNPs was calculated approximately as (1/12) of its LD50 value, which was 1 mg/kg body weight.

Experimental Animals

Six weeks old male albino rats (120-150g), obtained from the Egyptian Holding Company for Biological Products and Vaccines were used as experimental animals. Animals were kept under standard conditions of temperature and humidity along the experimental period. The rats were fed on standard pellets of a concentrated diet containing all the necessary nutritive elements. Liberal water intakes were available. Animal procedures were performed in accordance with the Ethics Committee of the National Research Centre and in accordance with the recommendations for the proper care and use of laboratory animals.

Animal groups

Animals were randomly distributed into 4 groups (10 rats / group). The period of experimental was extended to 12 weeks. Administration of DEN at the dose (20 mg/kg.b.wt.; orally; 5 times/week for 6 weeks) (Darwish and El-Boghdady, 2011) is zero time of experimental, treatment with GaNPs at a dose (1mg/Kg) starting from 7th week until the 12th week end of the experimental. The groups of animals were divided as follows: Control group: served as normal rats just received distil water by gavages, DEN Group: rats received DEN, GaNPs Group: rats treated with GaNPs, and DEN+GaNPs group: rats were orally administrated with DEN and GaNPs.

After 12 weeks, rats of each group have fasted overnight before the time of sacrificing. Serum was obtained from each group. The whole liver and brain of animals in each group was quickly removed. Liver tissues were washed with ice-cold saline and fixed in 10% formalin and embedded in paraffin for histological examination. Brain tissues were snap-frozen directly in liquid nitrogen and stored at -80°C for biochemical investigation.

Biochemical Assay

In brain tissue, Lipid peroxidation was measured by thiobarbituric acid assay, which is based on malonaldehyde (MDA) reaction with thiobarbituric acid forming thiobarbituric acid reactive substances (TBARS), a pink color complex exhibiting a maximum absorption at 532 nm according to Yoshioka et al., (1979). Reduced glutathione (GSH) content was determined photometrically at 412 nm using 5, 5-dithiobis-2-nitrobenzoic acid (Ellman, 1959). Glutathione-S-transferase (GST) catalyzes the conjugation reaction with glutathione in the first step of mercapturic acid synthesis according to the method of Habig and Jakoby, (1974). Vascular endothelial growth factor (VEGF) and vascular cells adhesion molecule-1 (VCAM-1) were detected by ELISA kit supplied by R and D System USA after following the manufacturer's instruction. In serum, alpha-fetoprotein was estimated by enzyme-linked immunosorbent assay (ELISA) using a rat alpha-fetoprotein (AFP) ELISA kit purchased from Glory Science Co., Ltd (USA). Activities of serum alanine aminotransferase (ALT) and aspartate aminotransferase (AST) were determined colorimetrically according to Reitman and Frankel, (1957). Serum gamma-glutamyl transferase (GGT) activity was measured kinetically according to Szasz, (1976).

Detection of CYT P450 and BSSP4 gene expression by quantitative real time PCR RNA isolation and reverse transcription

RNA was extracted from the tumor tissue homogenate using the RNeasy plus mini kit (Qiagen, Venlo, The Netherlands), according to the manufacturer's instructions. Genomic DNA was eliminated by a DNase-on-column treatment supplied with the kit. The RNA concentration was determined spectrophotometrically at 260 nm using the NanoDrop ND-1000 spectrophotometer (Thermo Fisher scientific, Waltham, USA) and RNA purity was checked by means of the absorbance ratio at 260/280 nm.

RNA integrity was assessed by electrophoresis on 2% agarose gels. RNA (1 µg) were used in the subsequent cDNA synthesis reaction, which was performed using the Reverse Transcription System (Promega, Leiden, The Netherlands). Total RNA was incubated at 70°C for 10 min to prevent secondary structures. The RNA was supplemented with MgCl₂ (25mM), RTase buffer (10X), dNTPmixture (10mM), oligod (t) primers, RNase inhibitor (20 U) and AMV reverse transcriptase (20 U/µl). This mixture was incubated at 42°C for 1 h.

Quantitative real time PCR: qRT-PCR was performed in an optical 96-well plate with an ABI PRISM 7500 fast sequence detection system (Applied Biosystems, Carlsbad, California) and universal cycling conditions of 40 cycles of 15 s at 95°C and 60 s at 60°C after an initial denaturation step at 95°C for 10 min. Each 10 µl reaction contained 5 µl SYBR Green Master Mix (Applied Biosystems), 0.3 µl gene-specific forward and reverse primers (10 µM), 2.5 µl cDNA and 1.9 µl nuclease-free water. The sequences of PCR primer pairs used for each gene are shown in Table 1. Data were analysed with the ABI Prism sequence detection system software and quantified using the v1.7 Sequence Detection Software from PE Biosystems (Foster City, CA). Relative expression of studied genes was calculated using the comparative threshold cycle method. All values were normalized to the endogenous control GAPDH (Livak and Schmittgen, 2001).

Western blot analysis of Tau and ERK-1

Part of brain tissue was homogenized with RIPA buffer containing 5 M NaCl, 1 mM phenylmethylsulfonyl fluoride (PMSF), 10% deoxycholic acid (DOC), 10% SDS, 1 M Tris (pH 8.6). The tissue lysate was centrifuged at 12000 rpm for 20 min at 4°C. The lysate was then collected and protein concentration was determined with a BCA protein assay kit (Thermo Fisher Scientific Inc., USA). An aliquot of 7.5 µg protein of each sample was denatured, then each sample was loaded on 8% sodium dodecyl sulphate-polyacrylamide gel electrophoresis (PAGE) and transferred to a nitrocellulose membrane (Amersham Bioscience, Piscataway, NJ, USA) using a semidry transfer apparatus (Bio-Rad, Hercules, CA, USA). The membranes were incubated with 5% milk blocking buffer containing 10 mM Tris-HCl (pH 7.4), 150 mM NaCl, and Tris-buffered saline with 0.05% Tween-20 (TBST) at 4°C overnight. The membranes were then washed with TBST and incubated with a 1:1,000 dilution of anti-tau (phosphorylated) or anti-ERK-1 (phosphorylated) (Thermo Fisher Scientific Inc., USA) for overnight on a roller shaker at 4°C. The filters were washed and subsequently probed with horseradish peroxidase-conjugated goat anti-mouse immunoglobulin (Amersham. Life Science Inc., USA). Chemiluminescence detection was performed with the Amersham detection kit according to the manufacturer's protocols and exposed to X-ray film. The amount of study protein was quantified by densitometric analysis of the autoradiograms using a scanning laser densitometer (Biomed Instrument Inc., USA). Results were expressed after normalization for β-actin protein expression (as housekeeping protein) (Mingone et al., 2003).

Histopathological study

Autopsy samples were taken from the liver of rats of different groups and fixed in 10% formalin saline for twenty-four hours. Washing was done with tap water, then serial dilutions of alcohol (methyl, ethyl, and absolute ethyl) were used for dehydration. Specimens were cleared in xylene and embedded in paraffin at 56 degrees in hot air oven for twenty-four hours. Paraffin beeswax tissue blocks were prepared for sectioning at 4 microns thickness by slide microtome. The obtained tissue sections were collected on glass slides, deparaffinized, and stained with hematoxylin and eosin stain for routine examination through the light electric microscope (Banchroft et al., 1996).

Statistics

Statistical analysis was performed by one way analysis of variance (ANOVA) followed by Duncan's Multiple Range test by using statistical package of social science (SPSS) version 15.0 for windows. P ≤ 0.05 were considered as a level of significance.

Results

Verification of GaNPs

By FT-IR technique

The FT-IR analysis of the extracellular extract of *Bacillus licheniformis* (Figure 1A), which used for GaNPs green synthesis, and GaNPs (Figure 1B) showed different stretches of bonds at different peaks (Figure 1). FT-IR spectra of the broth contains bacteria extracellular metabolites showed major strong peaks and some weak bonds, a strong signal at 3318.77cm⁻¹ (represents a hydroxyl group), strong signal at 1,636.93 cm⁻¹ (represents amide I bond of proteins), and a strong peak at 602.31 cm⁻¹ (represents signal bond of C-H, C-N bonds).

The FT-IR analysis of GaNPs showed shifting in wave number representing -OH group at 3321.45 cm⁻¹, also in the signal of amide I of proteins at 1637.29 cm⁻¹, and at 595.64 cm⁻¹ the signal of C-H, C-N bonds. The shifting

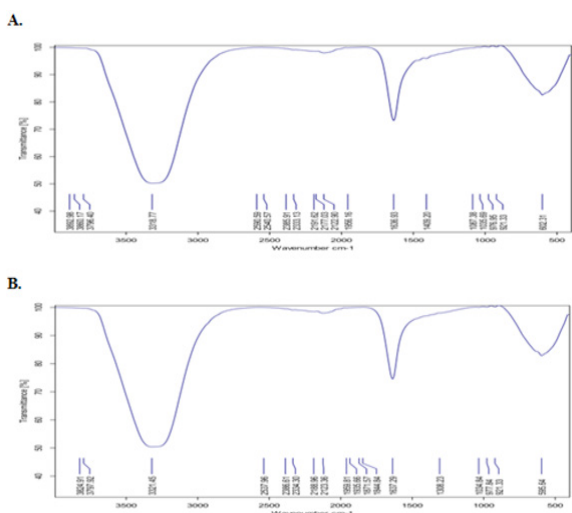


Figure 1. FTIR Analysis of GaNPs Showing Different Stretches of Bonds Shown at Different Peaks. A) extracellular extract of *Bacillus licheniformis* and B) GaNPs formation

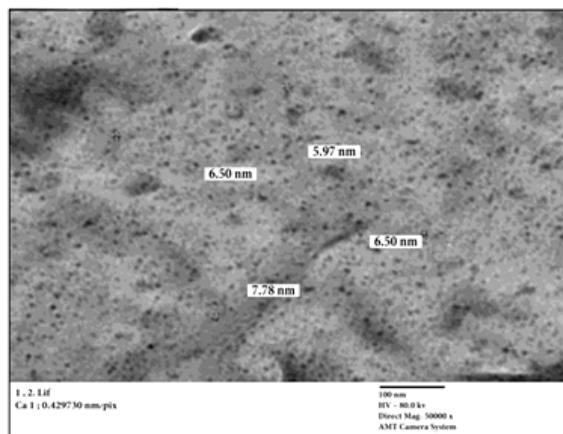


Figure 2. TEM Image of GaNPs Showing Nanoparticles of Spherical Shape with Diameter Range between 5 and 7 nm

in FT-IR spectra indicates the involve of functional groups in the extracellular metabolites of bacteria in GaNPs formation as a reducing agents, reduced Ga²⁺ to Ga⁰. The oxidized group caused signal shifting. This confirmed the presence of bioactive molecules and their adsorption onto GaNPs coating Ga ions results in stable structure of the nanoparticles.

By TEM technique

In the current study, TEM micrograph of GaNPs was displayed nanoparticles with spherical shape and particle sizes ranging from 5-7 nm, with a relatively narrow particle size distribution (Figure 2).

Verification of HCC induction

Liver function and alpha-fetoprotein

Data from Table (2) represent liver function enzymes

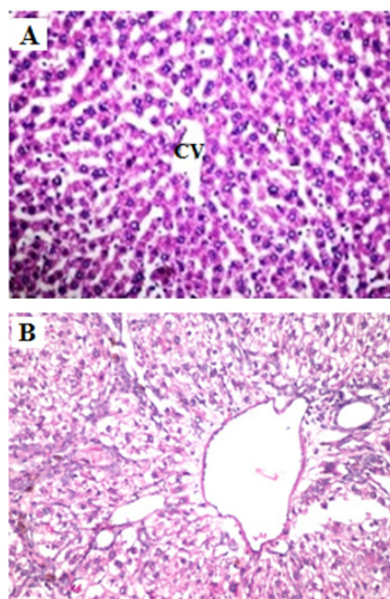


Figure 3. Histopathological Examination of Liver. (A) Normal liver histology of a rat fed the standard diet. (B) Rats administrated DEN display focal area of anaplastic hepatocytes with other cells forming acini were observed associated with fibroblastic cells proliferation dividing the degenerated and necrosed hepatic parenchyma into nodules (H and E X400).

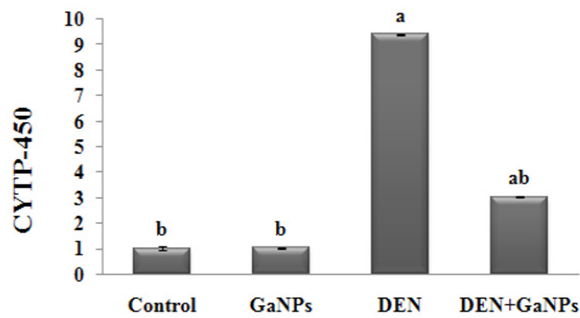


Figure 4. Effect of Ganps on Gene Expression of CYTP450 By qrt-PCR Analysis. Each value represents the mean \pm SE (n=6). a: significantly different from control at $p<0.05$. b: significantly different from DEN at $p<0.05$.

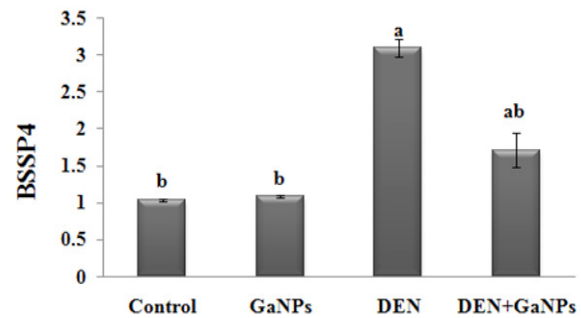


Figure 5. Effect of GanPs on Gene Expression of BSSP4 by qRT-PCR Analysis. Each value represents the mean \pm SE (n=6). a: significantly different from control at $p<0.05$. b: significantly different from DEN at $p<0.05$.

Table 1. Primer Sequences Used for RT-PCR

Primer	Sequence
CYT-P450	Forward 5'-ACTTCTACCTGCTGAGCAC-3'
	Reverse 5'-TTCAGGTCTCATGAACGGG-3'
BSSP4	Forward 5'-CTTCAAGCTCAAGAATGCCTATGA-3'
	Reverse 5'-TGCACATTTTTACCCCTTCTC-3'
GAPDH	Forward: 5'- CTCCCATTCTCCACCTTTG-3'
	Reverse: 5'- CTTGCTCTCAGTATCCTTGC-3'

(AST, ALT and GGT) and tumor marker AFP in serum. We showed that non-significant change was observed in GaNPs group compared to control group. While, after DEN administration, a significant increase was observed in liver enzymes and AFP compared to control group. Meanwhile, administration of GaNPs improved this elevation compared with DEN group.

Histopathological findings

Histopathological examination of liver sections of control rats showed normal hepatic architecture (Figure 3A). On the other hand, animals treated with DEN showed focal area of anaplastic hepatocytes with other cells forming acini were observed associated with fibroblastic cells proliferation dividing the degenerated and necrosed hepatic parenchyma into nodules (Figure 3B).

Effect of GaNPs on Brain Metastasis

CYTP450

Here, we investigated the effect of GaNPs on the

gene expression of CYTP450. The qRT-PCR analysis showed non-significant change in GN group compared to control group. On the other hand, our results provoked a significant elevation ($P<0.05$) in CYTP450 mRNA expression in DEN-group compared to the control (Figure 4). Moreover, we found that administration of GaNPs significantly improved CYTP450 gene expression in DEN+GaNPs group compared to the DEN group.

BSSP4

The qRT-PCR analysis demonstrated non-significant

Table 2. Effect of GaNPs on ALT, AST and GGT Liver Enzyme and AFP Tumor Marker in Serum

Animal groups	AST (U/L)	ALT (U/L)	GGT (U/L)	AFP (ng/ml)
Control	66 \pm 3.5 ^b	58.5 \pm 4.9 ^b	11.5 \pm 0.7 ^b	0.47 \pm 0.06 ^b
GaNPs	68 \pm 4.1 ^b	58.5 \pm 7.8 ^b	12.5 \pm 0.7 ^b	0.47 \pm 0.40 ^b
DEN	99 \pm 5.1 ^a	82.5 \pm 3.5 ^a	16.5 \pm 0.7 ^a	2.17 \pm 0.33 ^a
DEN+ GaNPs	73 \pm 3.8 ^b	65.5 \pm 3.5 ^b	13.5 \pm 0.7 ^b	0.41 \pm 0.03 ^b

Each value represents the mean \pm SE (n=6). a: Significant difference from control at $p<0.05$. b: Significant difference from DEN group at $p<0.05$.

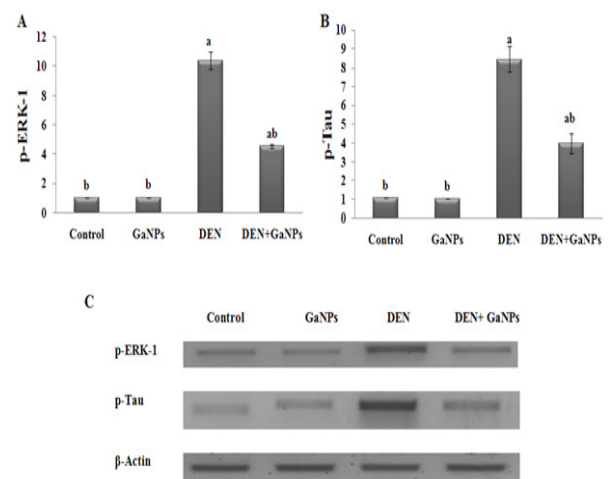


Figure 6. Effect of GaNPs on Protein Expression of A) p-ERK-1 and B) p-Tau by western blot analysis. C) PAGE of p-ERK-1 (44 kDa), p-Tau (64 kDa) proteins and β -actin (42 kDa) as housekeeping protein. Each value represents the mean \pm SE (n=6). a: significantly different from control at $p<0.05$. b: significantly different from DEN at $p<0.05$.

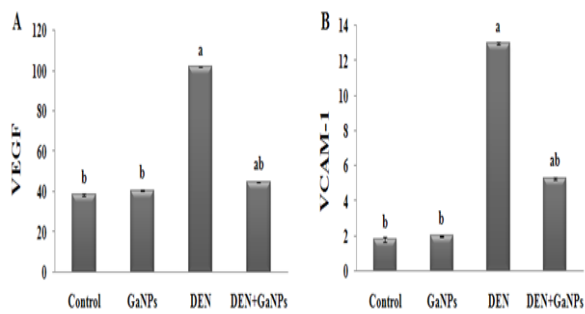


Figure 7. Effect of GaNPs on A) VEGF (pg/mg tissue) and B) VCAM-1 (pg/mg tissue) Levels. Each value represents the mean \pm SE (n=6). a: significantly different from control at $p < 0.05$. b: significantly different from DEN at $p < 0.05$.

change in mRNA expression gene of BSSP4 in GaNPs group compared to control group. In addition, we found that DEN results revealed a significant increase BSSP4 mRNA expression gene compared to the control group. Additionally, GaNPs treatment significantly decreased BSSP4 mRNA expression gene in DEN+GaNPs group compared to DEN results (Figure 5).

p-ERK-1 and p-Tau

Here, we measured p-ERK-1 (Figure 6A) and p-Tau protein (Figure 6B) secretion levels by performing Western blot assay. In GaNPs group, no significant change observed compared with control in p-ERK-1 and p-Tau protein secretion levels. From our data represented in (Figure 6), we found that the DEN induced significant elevation in protein expression of p-ERK-1 and p-Tau as compared with control. On the other hand, GaNPs treatment significantly reduced this elevation in DEN+GaNPs group compared to DEN group (Figure 6).

VEGF and VCAM-1

In GaNPs group, no significant change recorded in VEGF and VCAM-1 levels compared with control group (Figure 7). On the other side, DEN showed a significant increase in VEGF and VCAM-1 levels compared to the control group (Figure 7). From our data, we showed that the administration of GaNPs in DEN+GaNPs group significantly improve VEGF and VCAM-1 levels compared to DEN group (Figure 7).

MDA and GST

In this study, we set out to determine whether GaNPs can affect the oxidative stress in rats exposed to DEN. Compared to control group, the experimental data showed that the oxidative stress marker (MDA) and antioxidant enzyme (GST activity) was non-significantly change in GN group (Figure 8). In rats exposed to DEN, the results revealed oxidative stress status display by a highly significant ($P < 0.05$) in MDA levels (Figure 8A) concomitant with a significant decrease in GST activity (Figure 8B) compared to the control (Figure 8). GaNPs supplementation improved GST activity significantly in the DEN+GaNPs group compared to the DEN group. But, a significant elevation in MDA levels was displayed

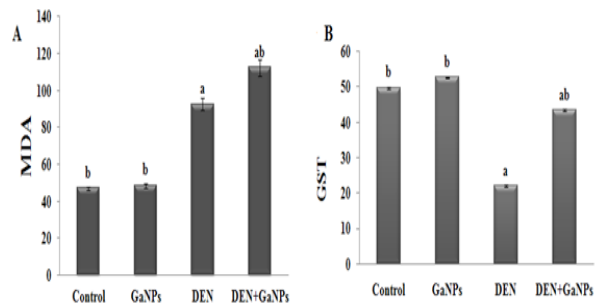


Figure 8. Effect of GaNPs on A) MDA (nmole/gm wet tissue) and B) GST (U/mg protein) levels. Each value represents the mean \pm SE (n=6). a: significantly different from control at $p < 0.05$. b: significantly different from DEN at $p < 0.05$.

compared to DEN group (Figure 8).

Discussion

Data in the current study demonstrate that administration of GaNPs nanoparticles significantly decrease BSSP4 mRNA gene expression, protein expression of p-ERK-1 and p-Tau secretion levels. Moreover, GaNPs reduced VEGF, VCAM-1 levels and significantly modulate CYTP450 gene expression compared to DEN group. Furthermore, GaNPs supplementation reduced MDA levels and improved GST activity in parallel with modulate liver enzyme levels (ALT, AST, and GGT) and inhibited tumor marker (AFP) compared to the DEN group.

In the present study reveal that, DEN-induced HCC. This was observed by increased serum levels of liver function enzymes (ALT, AST, and GGT) and AFP and focal area of anaplastic hepatocytes with fibroblastic cells proliferation dividing the degenerated and necrosed hepatic parenchyma into nodules were displayed in the histopathological examination of liver tissues. Such elevations in the transaminases are considered as the most sensitive markers in the diagnosis of hepatocellular damage and loss of functional integrity of the membrane which subsequently break down membrane architecture of the cells and leads to their spillage into serum where their concentration raises (Sayed-Ahmed et al., 2010; Hassan et al., 2014). Moreover, GGT elevation reveals cholestasis and bile duct necrosis. This significant elevation of GGT in serum may be attributed to its liberation from the plasma membrane into the circulation as it is located on the outer membrane of the hepatic cells, indicating damage of the cell membrane as a result of carcinogenesis (Hassan et al., 2014). This observed increase in liver function by DEN could be a secondary event following DEN-induced lipid peroxidation of hepatocyte membranes with the consequent increase in the leakage of enzymes from liver tissues by a production of reactive oxygen and nitrogen species. This action of DEN plays an important role in DEN-induced initiation of hepatic carcinogenesis (Sayed-Ahmed et al., 2010). AFP expression is induced in regenerating liver and liver tumors. DEN is a genotoxic carcinogen that has been shown to induce liver tumors and liver damage (Motalleb et al, 2008). In agreement with

Song et al., (2013), the present study showed a significant increase in the AFP level of DEN group (Table 2) this might be due to DEN intoxication that caused necrosis of the hepatocytes. Hepatocyte localization within the liver plate or outside it is the defining factor that regulates the activity of AFP synthesis on a cellular level (Motaleb et al, 2008). Changes occurring in the biochemical parameters were confirmed by the histopathological observation (Figure 1). This finding agrees with (Sindhua et al., 2013).

In our study, we found that significantly increased levels of CYP450 mRNA in DEN group compared with control. CYP450 which is one of phase I enzymes that are involved in the oxidative activation or deactivation of both endogenous and exogenous compounds such as drugs, environmental toxins and dietary constituents (Miksys and Tyndale, 2002). This increase in the expression might be due to its responsible for the functionalization of xenobiotics either by the introduction of a polar functional group or by the unmasking of a polar functionality. In addition, brain microsomes have been shown to metabolize the same probe substrates used to assess specific hepatic CYP activity (e.g., N-nitrosodimethylamine) (Miksys and Tyndale, 2002). Other potential toxicological consequences of the increase in the level of CYP450 in the brain are (i) an increase in the release of active oxygen and its attendant increase in lipid peroxidation and destruction of membranes that has been shown to occur with this isozyme of P450. Also, induction of this enzyme in the brain, increase the risk of neuronal damage (Warner and Gustafsson, 1994). Data from this study revealed that DEN significantly increased MDA and decreased GST activity in brain tissues (Figure 6). This is possibly due to N-nitrosamines which have received much attention as a potential risk factor for the brain tumor. Whereas, N-nitrosamines effects decreased antioxidant levels and this correlated with the severity of malignancy in brain tumors and with the formation of considerable amounts of oxidative stress products including the free radicals in brain tissues (Sheweita and Sheikh, 2011). Also, Sayed-Ahmed et al., 2010 found that significantly increased in MDA content and decreased in GST activity in DEN group attributed this increase to free radical production during DEN metabolism. Associated with the increase in ROS production, membrane lipid peroxidation and decrease of antioxidant, we found significantly increased in protein expression of Tau of DEN group. Whereas Naini and Soussi-Yanicostas, (2015) concluded that accumulation of hyperphosphorylated tau has been shown to cause oxidative stress, but ROS have also been shown to stimulate tau hyperphosphorylation. In addition, close interplay between tau hyperphosphorylation and oxidative stress suggests that these events are two key components of a vicious circle that play a crucial role in the pathologic process in tau pathologies. Furthermore, de la Monte et al., (2009) revealed relative increases in pTau in the DEN group and attributed this to DEN effect on impaired insulin/insulin growth factor signaling with cytoskeletal collapse and increased in oxidative stress status. Based on our observations, we can conclude that brain metastasis was arising from HCC. This finding agrees with Tunc et al., (2004) who reported that when

confronted with a patient with liver dysfunction and neurologic findings, the clinician must suspicion of such associations. On the other hand, our results showed that significantly increased in BSSP4 mRNA expression in DEN-group. This elevation might be attributed to DEN, being a genotoxic carcinogen, induced mutations associated with inflammatory response, immune response and oxidative stress which responsible for the development of hepatocarcinogenesis (Liu et al., 2009; Hassan et al., 2014). Subsequently, a significant increase in p-ERK protein expression, VEGF, and VCAM-1 levels were observed in DEN group. Whereas, Chen et al. (2014) conclude that the stimulation of ERK and VEGF expression is mediated via BSSP4. In addition, Kim et al. (2001) have demonstrated that VEGF-stimulate expression of intercellular adhesion molecule-1 (ICAM-1) and VCAM-1. Furthermore, Gupta et al., (1999) showed that the VEGF-induced activation of the ERK pathway. ERK kinases are frequently abnormally activated in most human cancers, leading to proliferation and acceleration of other oncogenic processes, such as angiogenesis and survival (Wei et al., 2011). Meanwhile, Kim and Choi, 2010 have reported that Tau in a hyperphosphorylated form in neurofibrillary tangles was mediated by several kinases including ERK.

In the present study, GaNPs synthesis by the strain *B. Licheniformis* formed reddish cell suspension, which indicated its ability to reduce the toxic, colorless, soluble gallium to nontoxic. Under the stressful condition of toxic gallium, the morphology of the cells was altered resulting in a decrease in cell size. The organisms reduce their cell size and increase their relative surface area for better uptake of the nutrients for survival under environmental stress conditions.

Brain tumors are generally either a primary brain tumor or a secondary metastasis from a distant primary tumor in another organ, our study is a novel strategy targeting Brain Specific Serine Protease-4 whereas BSSP4 has been shown to play a role in different cancers, few studies to date have focused on its specific function in cancer biology. To our knowledge, the role of GaNPs nanopartecals and underlying mechanism of inhibition of BSSP4 in brain tissue of hepatocellular carcinogenesis model are yet to be established. After administration of GaNPs, we found significant modulation in CYP450 and BSSP4 mRNA expression, p-ERK and P-Tau protein expression and subsequently in VEGF and VCAM-1 levels. This modulation could be attributed to Ga which modifies the three-dimensional structure of DNA and inhibits its synthesis, modulates protein synthesis, inhibits the activity of a number of enzymes, such as ATPases, DNA polymerases, ribonucleotide reductase and tyrosine-specific protein phosphatase (Collery et al., 2002). Accordingly, the elevation observed in MDA levels after GaNPs could be ascribed to Liao, (2015) who found that MDA (the production of lipid peroxidation) may be one of the mechanisms for gallium-related DNA damage in multiple regression models. Also, we found a significant increase in GST activity, which is one of phase II detoxification enzymes, this might be due to Yang and Chitambar, (2008) who suggested that exposure of cells

to gallium nitrate triggers signaling through the p38 MAP kinase pathway which leads to the activation of Nrf2 and transcription of the HO⁻¹ gene. Whereas, NF-E2-related factor 2 (NRF2) regulates a battery of antioxidative and phase II drug metabolizing/detoxifying genes through binding to the antioxidant response elements (Huang et al., 2012).

In conclusion, the present study shed lights on the therapeutic role of GaNPs against brain metastasis arising from HCC induced experimentally by diethylnitrosamine. Based on our results, we can conclude that the gaps mechanism of DNA damage could prevent metastasis and the development of cancer. Whereas, GaNPs inhibit CYP450 and BSSP4 mRNA expression, then this subsequently down-regulate protein expression of p-ERK, P-Tau, and reduce levels of angiogenesis process markers (VEGF and VCAM-1). So, we can recommend GaNPs as anti-metastasis due to its modulates to protein synthesis, inhibits the activity of a number of enzymes involved in gene expression and its anti-angiogenic effect.

Declaration of Interests

The authors stated that they have no conflicts of interest regarding the publication of this article.

Acknowledgments

Authors acknowledge Dr. Sawsan M. El-Sonbaty (Health Radiation Research Department, NCCRT, Atomic Energy Authority, Egypt) for nanoparticles gallium preparation and Dr. Adel Bakeer Kholoussy Prof. of Pathology, Faculty of Veterinary Medicine, Cairo University for the performing of histopathological examination.

References

Antalis T, Bugge T, Wu Q (2011). Membrane-anchored serine proteases in health and disease. *Prog Mol Biol Transl Sci*, **99**, 1-50.

Banchroft J, Stevens A, Turner D (1996). Theory and practice of histological techniques. 4th Churchil Livingstone, New York, London, San Francisco, Tokyo. P, 273-92

Bonchi C, Imperi F, Minandri F, Visca P, Frangipani E (2014). Repurposing of gallium-based drugs for antibacterial therapy. *Biofactors*, **40**, 303-12.

Chen C-Y, Chung I-H, Tsai M-M, et al (2014). Thyroid hormone enhanced human hepatoma cell motility involves brain-specific serine protease 4 activation via ERK signaling. *Mol Cancer*, **13**, 162.

Chitambar C (2010). Medical applications and toxicities of gallium compounds. *Int J Environ Res Public Health*, **7**, 2337-61.

Collery P, Keppler B, Madoulet C, Desoize B (2002). Gallium in cancer treatment. *Crit Rev Oncol Hematol*, **42**, 283-96.

Darwish H, El-Boghdady N (2011). Possible involvement of oxidative stress in diethylnitrosamine induced hepatocarcinogenesis: chemopreventive effect of curcumin. *J Food Biochem*, **37**, 353-61.

de la Monte SM, Tong M, Lawton M, Longato L (2009). Nitrosamine exposure exacerbates high fat diet-mediated type 2 diabetes mellitus, non-alcoholic steatohepatitis, and neurodegeneration with cognitive impairment. *Mol*

Neurodegener, **4**, 54.

Ellman G (1959). Tissue sulfhydryl groups. *Arch Biochem Biophys*, **82**, 70-7.

Espey M, Miranda K, Thomas D et al (2002). A chemical perspective on the interplay between NO, reactive oxygen species, and reactive nitrogen oxide species. *Ann N Y Acad Sci*, **962**, 195-206.

Gupta K, Kshirsagar S, Li W, et al (1999). VEGF prevents apoptosis of human microvascular endothelial cells via opposing effects on MAPK/ERK and SAPK/JNK signaling. *Exp Cell Res*, **247**, 495-504.

Habig, W, Jakoby, W (1974). Glutathione s transferases. the first enzymatic step in mercapturic acid formation. *J Biol Chem*, **249**, 7130-139.

Hassan S, Mousa A, Esha M, et al (2014). Therapeutic and chemopreventive effects of nano curcumin against diethylnitrosamine induced hepatocellular carcinoma in rats. *Int J Pharm Pharm Sci*, **6**, 54-62.

Hodgson EA (2010). textbook of modern toxicology. 4th ed. Hoboken: John Wiley and Sons, Inc, p 672.

Holt J, Krieg R, Sneath P, et al (1994). Bergey's Manual of Determinative Bacteriology, 9th ed., Williams and Wilkins, Baltimore. 816

Huang Y, Li W, Kong A-N (2012). Anti-oxidative stress regulator NF-E2-related factor 2 mediates the adaptive induction of antioxidant and detoxifying enzymes by lipid peroxidation metabolite 4-hydroxynonenal. *Cell Biosci*, **2**, 40.

Huang B, Zhang J, Hou J, Chen C (2003). Free radical scavenging efficiency of nano-Se in vitro. *Free Radic Biol Med*, **35**, 805-13.

Kim E, Choi E-J (2010). Review pathological roles of MAPK signaling pathways in human diseases. *Biochim et Biophys Acta*, **1802**, 396-405.

Kim I, Moon SO, Kim SH, et al (2001). Vascular endothelial growth factor expression of intercellular adhesion molecule 1 (ICAM-1), vascular cell adhesion molecule 1 (VCAM-1), and E-selectin through nuclear factor-kappa B activation in endothelial cells. *J Biol Chem*, **276**, 7614-20.

Kohno M, Tanimura S, Ozaki K (2011). Targeting the extracellular signal-regulated kinase pathway in cancer therapy. *Biol Pharm Bull*, **34**, 1781-4.

Lester-Coll N, Rivera E, Soscia S, et al (2006). Intracerebral streptozotocin model of type 3 diabetes: relevance to sporadic Alzheimer's disease. *J Alzheimers Dis*, **9**, 13-33

Liao Y-H (2015). Effects of gallium, indium, and arsenic dose biomarkers and malondialdehyde on zinc protoporphyrin and DNA fragments in optoelectronic workers. *Int J of Health*, **3**, 24-8.

Lijinsky W (1999) N-Nitroso compounds in the diet. *Mutat Res*, **443**, 129-38.

Liu YF, Zha BS, Zhang HL, et al (2009). Characteristic gene expression profiles in the progression from liver cirrhosis to carcinoma induced by diethylnitrosamine in a rat model. *J Exp Clin Cancer Res*, **28**, 107.

Livak KJ, Schmittgen T (2001). Analysis of relative gene expression data using real-time quantitative PCR and the 2^{-2DDCT}. *Methods*, **25**, 402-8.

Matsui H, Kimura A, Yamashiki N, et al (2000). Molecular and biochemical characterization of a serine proteinase predominantly expressed in the medulla oblongata and cerebellar white matter of mouse brain. *J Biol Chem*, **275**, 11050-7.

Miksyz S, Tyndale R (2002). Drug-metabolizing cytochrome P450s in the brain. *J Psychiatry Neurosci*, **27**, 406-15.

Mingone C, Gupte S, Quan S, et al (2003). Influence of heme and heme oxygenase-1 transfection of pulmonary microvascular endothelium on oxidant generation and cGMP. *Exp Biol*

- Med Maywood*, **228**, 535–9.
- Mohanraj V, Chen Y (2006). Nanoparticles – A review. *J Pharm, Res*, **5**, 561.
- Motalleb G, Hanachi P, Fauziah O, Asmah R (2008). Effect of berberis vulgaris fruit extract on alpha-fetoprotein gene expression and chemical carcinogen metabolizing enzymes activities in hepatocarcinogenesis rats. *Iran J Cancer Prev*, **1**, 33-44.
- Nagavarma B, hemant K, ayaz A, et al (2012). Different techniques for preparation of polymeric nanoparticles- a review. *Asian J Pharm Clin Res*, **5**, 16-23.
- Naini S, Soussi-Yanicostas N (2015). Tau hyperphosphorylation and oxidative stress, a critical vicious circle in neurodegenerative tauopathies?. *Oxid Med Cell Longev*, Article ID 151979.
- Park E, Kwon D, Park J, et al (2014). Gamma Knife surgery for treating brain metastases arising from hepatocellular carcinomas. *J Neurosurg*, **12**, 102–9.
- Pegg AE (1980). Metabolism of N-nitrosodimethylamine. *IARC Sci Publ*, pp 3–22.
- Philip D (2009). biosynthesis of Au, Ag and Au-Ag nanoparticles using edible mushroom extract. *Spectrochim Acta A Mol Biomol Spectrosc*, **73**, 374-81.
- Rajan B, Ravikumar R, Premkumar T, Devaki T (2015). Carvacrol attenuates N-nitrosodiethylamine induced liver injury in experimental Wistar rats. *Food Science and Human Wellness*, **4**, 66–74.
- Reitman S, Frankel S (1957). Colorimetric method for the determination of serum glutamic oxalacetic and glutamic pyruvic transaminases. *Am J Clin Pathol*, **28**, 56-63.
- Sayed-Ahmed M, Aleisa A, Al-Rejaie S, et al (2010). BioscienceThymoquinone attenuates diethylnitrosamine induction of hepatic carcinogenesis through antioxidant signaling. *Oxid Med Cell Longev*, **3**, 254-61.
- Sheweita SA, Sheikh B Y (2011). Can dietary antioxidants reduce the incidence of brain tumors?. *Curr Drug Metab*, **12**, 587-93.
- Sindhua E, Firdousa A, Ramnathb V, Kuttana R (2013). Effect of carotenoid lutein on N-nitrosodiethylamine-induced hepatocellular carcinoma and its mechanism of action. *Eur J Cancer Prev*, **22**, 320–27.
- Song Y, Jin SJ, Cui LH, et al (2013). Immunomodulatory effect of Stichopusjaponicus acid mucopolysaccharide on experimental hepatocellular Carcinoma in Rats. *Molecules*, **18**, 7179-93.
- Szasz G (1976). Reaction-rate method for gamma glutamyltransferase activity in serum. *J Clin Chem*, **22**, 2051.
- Szkudelski T (2001). The mechanism of alloxan and streptozotocin action in B cells of the rat pancreas. *Physiol Res*, **50**, 537–46.
- Tunc B, Filik L, Tezer-Filik I, Sahin B (2004). Brain metastasis of hepatocellular carcinoma: A case report and review of the literature. *World J Gastroenterol*, **10**, 1688-9.
- Warner M, Gustafsson J (1994). Effect of ethanol on cytochrome P450 in the rat brain. *Proc Natl Acad Sci USA*, **91**, 1019-23.
- Wei F, Yan J, Tang D (2011). Extracellular signal-regulated kinases modulate dna damage response - a contributing factor to using mek inhibitors in cancer therapy. *Curr Med Chem*, **18**, 5476–82.
- Yang M, Chitambar C (2008). Role of oxidative stress in the induction of metallothionein-2a and heme oxygenase-1 gene expression by the antineoplastic agent gallium nitrate in human lymphoma cells. *Free Radic Biol Med*, **45**, 763–72.
- Yasuda S, Morokawa N, Wong G, et al (2005). Urokinase-type plasminogen activator is a preferred substrate of the human epithelium serine protease tryptase epsilon/PRSS22. *Blood*, **105**, 3893–3901.
- Yoshioka T, Kawada K, Shimada T, Mori M (1979). Lipid peroxidation in maternal and cord blood and protective mechanism against activated-oxygen toxicity in the blood. *Am J Obstet Gynecol*, **135**, 372-76.